Soft Matter

Single-stranded DNA oligomer brush structure is dominated by intramolecular interactions mediated by the ion environment

Journal:	*Soft Matter*
Manuscript ID	SM-ART-08-2018-001743.R2
Article Type:	Paper
Date Submitted by the Author:	11-Nov-2018
Complete List of Authors:	Gil, Phwey; Case Western Reserve University, Chemical and Biomolecular Engineering Lacks, Daniel; Case Western Reserve University, Chemical Engineering Parisse, Pietro; INSTM-ST Unit; Elettra Sincrotrone Trieste SCpA Casalis, Loredana; Elettra Sincrotrone Trieste SCpA, NanoInnovationLab Nkoua Ngavouka, Maryse Dadina; Sincrotrone Trieste SCpA; Université Marien Ngouabi, Faculté des Sciences et Techniques, Physics; Institut National de Recherche en Sciences Exactes et Naturelles

Soft Matter

ARTICLE

Single-stranded DNA oligomer brush structure is dominated by intramolecular interactions mediated by the ion environment

Received 00th January 20xx,
Accepted 00th January 20xx

DOI: 10.1039/x0xx00000x

www.rsc.org/

Phwey S. Gil[a], Daniel J. Lacks[a] , Pietro Parisse[b,c] , Loredana Casalis[b,c], and Maryse D. Nkoua Ngavouka[c,d,e]*

Single-stranded DNA (ssDNA) brushes, in which ssDNA oligomers are tethered to surfaces in dense monolayers, are being investigated for potential biosensing applications. The structure of the brush can affect the selectivity and the hybridization efficiency of the device. The structure is commonly thought to result from the balance of intramolecular interactions, intermolecular interactions within the monolayer, and molecule-surface interactions. Here, we test the hypothesis that ssDNA oligomer brush structure is dominated by intramolecular interactions. We use AFM to measure the height of an ssDNA brush and molecular dynamics to simulate the end-to-end distance, both as a function of ionic strength of the surrounding solution. The brush height and the molecule end-to-end distance match quantitatively, providing evidence that the brush structure is dominated by intramolecular interactions (mediated by ions). The physical basis of the intramolecular interactions is elucidated by the simulations.

Introduction

Our knowledge of human genetics and its relation to human metabolism is developing with increasing momentum. With these developments comes the demand for devices that are capable of detecting key biological molecules (e.g. target nucleic acid sequences) with high specificity, quick assay times, low-cost, and other engineering challenges.

With our understanding of how two complementary single-stranded DNA (ssDNA) molecules hybridize into double-stranded DNA, we can envision that biosensors utilizing this mechanism can offer the specificity required for detecting target nucleic acids. Researchers have built biosensors based on this idea, where they have tethered short ssDNA molecules (15-40 bases long) to a surface to serve as binding sites for target nucleic acids.[1] The ssDNA molecules can be grafted to the surface as a high-density monolayer referred to as an ssDNA brush. The type of surface used, the monolayer density of the tethered ssDNA molecules, and the concentrations of salts may all affect the conformation of the probe ssDNA molecules, thereby affecting the selectivity and the hybridization efficiency of the device.[1]

The brush height is a key structural characteristic of polymer brushes, and it can be measured experimentally, for example, with AFM experiments. For brushes made of flexible polymer molecules, where the isolated molecule in solution takes on a coiled structure, the brush height is governed by a balance of entropic forces that act to coil the polymer, and enthalpic forces due to interactions of neighbouring molecules that act to partially uncoil the molecule.[2-9]

For brushes made of short ssDNA oligomers, however, the isolated molecule is more like a flexible rod than a coil, and thus the factors governing ssDNA brush height are different than those for flexible polymer brushes. For these ssDNA brushes, we expect the brush height to be governed by the length of individual molecules and their orientations with respect to the surface, as shown in **Fig. 1a**. For low density brushes, small constraining forces on each ssDNA molecule allow the molecules to take on a high entropy structure of random orientations, which leads to a low brush height (**Fig. 1b**). In contrast, for high density brushes, the large constraining forces from neighbouring molecules cause the ssDNA molecules to stand nearly fully upright, which leads to a higher brush height (**Fig. 1c**). Our previous AFM results on ssDNA brushes exhibited increasing brush height with increasing brush density, which can be attributed to the orientation effect shown in **Fig. 1**.[10] Moreover, experiments on double-stranded brushes show that above a certain brush density, the brush height becomes independent of the brush density (at a given ionic strength) – this result can be attributed to there being no further orientation effect once the molecules are fully upright.[11] We will refer to this regime, in which the molecules are oriented nearly fully upright, as the high-density regime.

In the high-density regime, the brush height will be dominated by the length of the molecules, as seen in **Fig. 1c,d**. Various factors can affect the ssDNA length, including interactions with the solvent and with other ssDNA molecules. Previous work has shown that ssDNA conformations, and thus

[a] Department of Chemical and Biomolecular Engineering, Case Western Reserve University, OH 441060 Cleveland, USA.
[b] INSTM-ST Unit, Strada Statale 14-km 163,5 in AREA Science Park, I-34149, Basovizza Trieste, Italy
[c] Elettra-Sincrotrone Trieste, S.C.p.A., Strada Statale 14-km 163,5 in AREA Science Park, I-34149, Basovizza Trieste, Italy
[d] Department of Physics, Université Marien Ngouabi, Faculté des Sciences et Techniques, 69 Brazzaville, Congo
[e] Institut National de Recherche en Sciences Exactes et Naturelles, Avenue de l'auberge Gascogne, Cité Scientifique, (Ex-OROSTOM), Château d'eau, Brazzaville, Congo

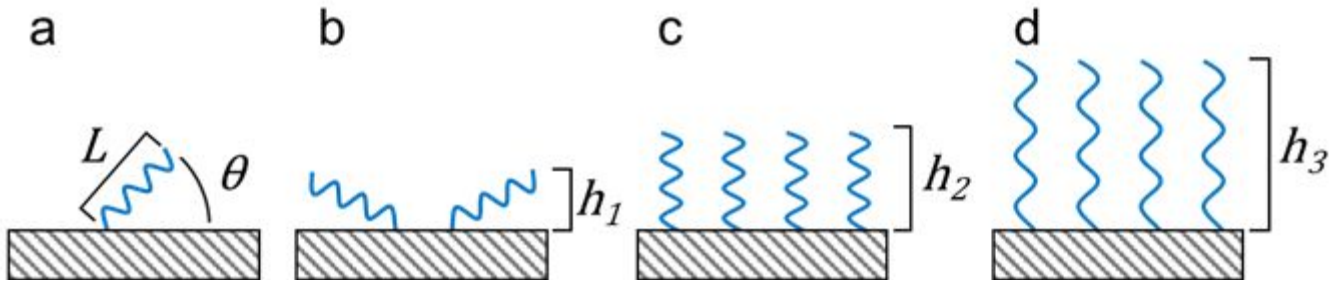

Fig. 1 The height of a brush composed of flexible rod-like molecules tethered to the surface depends on both **(a)** the molecule's length (L) and orientation (θ). **(b)** A brush composed of un-oriented molecules. **(c)** A brush with the molecules the same length as in b, but now oriented. (**d**) An oriented brush composed of molecules with a longer length.

their end-to-end lengths, are strongly dependent on the types and the concentrations of salt in the solution. This dependence is due to the highly charged backbone of an ssDNA molecule and the screening of electrostatic effects by the salts.[12-15]

The present study focuses on the height of brushes made from short ssDNA oligomers. We focus on the high-density regime, and aim to identify which factor – ssDNA-surface interactions, ssDNA-ssDNA interactions within the monolayer, or intramolecular interactions within individual ssDNA molecules – dominates the brush height in this regime. We hypothesize that intramolecular interactions mediated by salts in the solution dominate the structure. This hypothesis is tested by comparing results of AFM experiments for the heights of ssDNA brushes, with molecular dynamics simulations of free ssDNA molecules in solution.

In order to isolate the effects of molecular length from orientation effects in our AFM experiments, the AFM experiments address the high-density regime where the molecules are oriented nearly fully upright (as in **Fig. 1c,d**).

Methods

Experimental

We prepared a self-assembled monolayer of top oligo ethylene-glycol-terminated alkylthiols ($TOEG_6$, Sigma Aldrich) on a freshly cleaved, ultra-flat gold surface. We then operated the AFM cantilever at high load to replace a square 1 μm^2 area of $TOEG_6$ with thiolated ssDNA ($SH\text{-}(CH_2)_6\text{-}5'$-TAATCGGCTCATACTCTGACTG-3', Biomers GmbH - HPLC purification grade). This procedure, called nanografting, yields ssDNA nanobrushes of controllable density in the range ~$(1.3–1.8)x10^{13}$ molecules/cm^2; the procedure is described in more detail elsewhere.[10,15,16] The corresponding surface density was estimated according to the brush topographic height, via the procedure implemented by Bosco *et al.*[16]

We carried out atomic force microscopy (AFM, XE-100 PARK) to image this surface at low load (about 0.1 nN) in various concentrations of NaCl (0.001, 0.01, 0.1, and 1 M) with Tris EDTA (TE) buffer. Because the ssDNA nanostructure is embedded inside a $TOEG_6$ SAM, the zero of the AFM scan is taken as the height of the $TOEG_6$ layer. **Fig. 2a** shows the height profiles (relative to the $TOEG_6$ layer) and **Fig. 2b** shows the topography images at the different salt concentrations. The topography shows the square-shaped ssDNA area and the surrounding $TOEG_6$ carpet. To obtain the actual height of the ssDNA monolayer, the height of the $TOEG_6$ layer[10] (2.4 ± 0.3

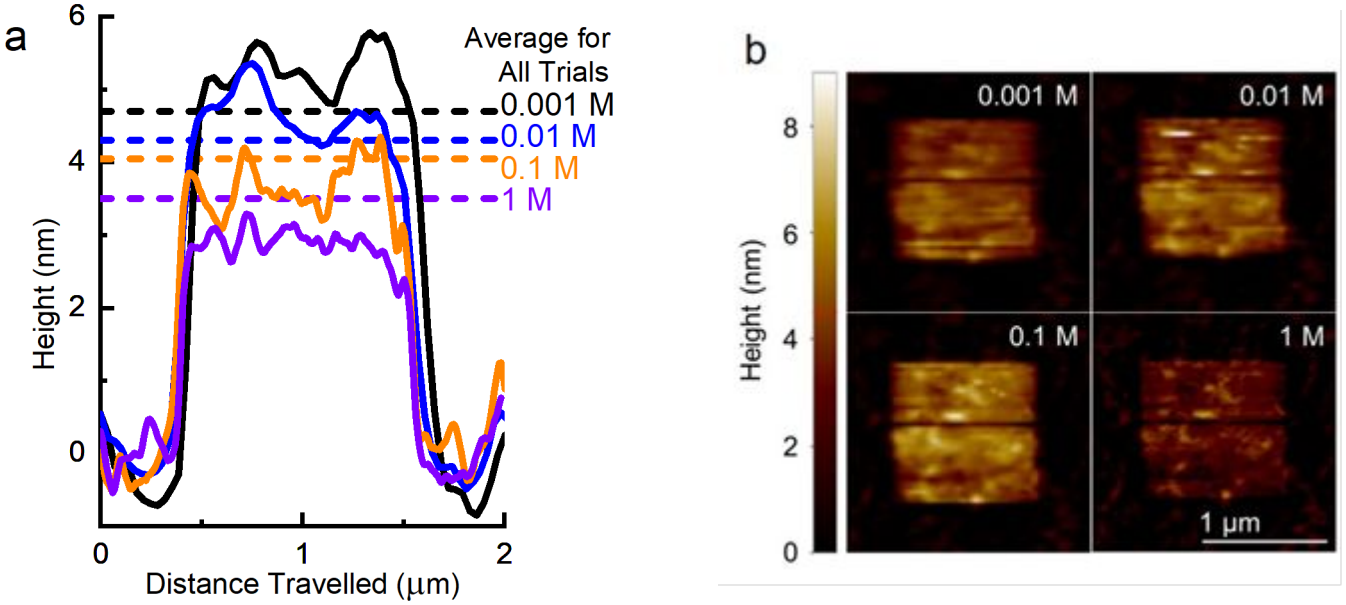

Fig. 2 **(a)** The height profile of the surface, relative to the $TOEG_6$ layer, at different concentrations of salt at 0.001 M (solid black line), 0.01 M (dotted blue line), 0.1 M (solid orange line), and 1 M (dotted purple line). **(b)** The AFM images of the surface at different concentrations of salt.

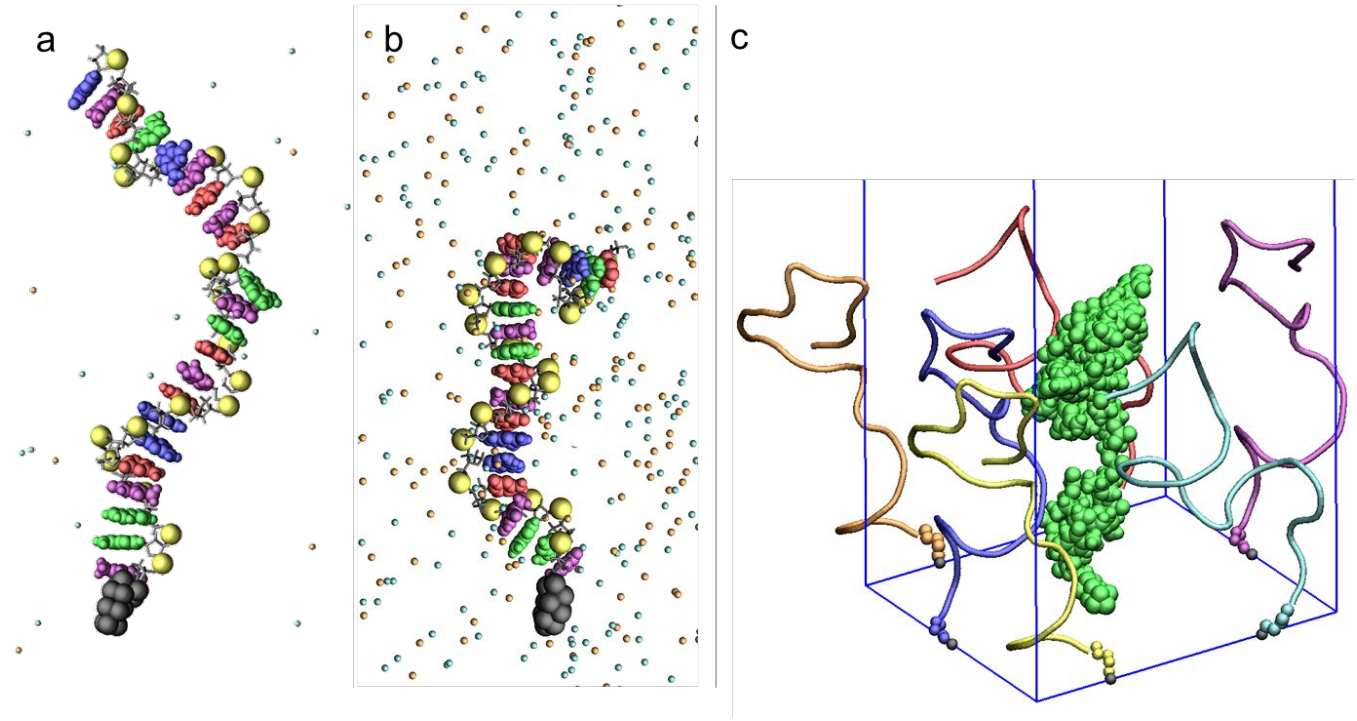

Fig. 3 Snapshots of the simulation trajectory of **(a)** a free ssDNA molecule in 0.02 M NaCl, **(b)** a free ssDNA molecule in 1.1 M NaCl, and **(c)** ssDNA molecules in a hexagonal lattice in 0.9 M NaCl, with ions omitted for clarity. The snapshots are centred and zoomed-in around the ssDNA, and do not show the entire simulation box. The Na+ ions are cyan and the Cl- ions are orange. The ssDNA backbone is grey, the C6 group is black, PO4- groups are yellow, adenine is green, thymine is purple, guanine is blue, and cytosine is red. Water molecules are not shown. The DNA end-to-end distance is defined as the distance between the 3' terminal oxygen (top) and the last tip of the C6 group (bottom). In (c), the backbones of individual ssDNA strands are shown as tubes of various colours except the centre strand where all of the atoms are shown.

nm) is added to the results in **Fig 2a**. Thus we find that the height of the ssDNA monolayer of **Fig. 2** is 7.1 ± 0.25 nm at low salt concentration, and then deceases with increasing salt concentration. Due to the helical structure of the ssDNA, these heights are approximately half of the height that would be found if the ssDNA were fully extended, since the DNA contour length is approximately 0.63 nm per base.[12]

Simulation

We carried out molecular dynamics simulations of a free ssDNA molecule in solution, at the infinite dilution limit. Molecular dynamics is a method for simulating the movement of atoms in a system. Numerical solutions to Newton's Laws of Motion yield the trajectory of the atoms interacting via interatomic forces defined through a set of mathematical definitions called a force-field. The trajectory can be analysed to give macroscopic properties of the system or to give insights into various physical mechanisms. We used the parmbsc1 force-field[17] optimized for DNA simulations, the SPC/E force-field[18] for water molecules, and the Na+ and Cl- ions were simply treated as charged Lennard-Jones particles.[19] To simulate equilibrium conditions, we ran simulations at fixed volume and temperature.[20] The temperature was controlled at 300 K by the velocity-rescaling thermostat[21] with a time constant of 1 ps. The short-range (< 1 nm) Van der Waals and electrostatic interactions were computed directly in real space, and the long-range (> 1 nm) interactions were computed using the Particle-Mesh-Ewald method.[22]

The system included one 22-base ssDNA molecule with a 6-carbon linker [(CH_3) $(CH_2)_5$-5'-TAATCGGCTCATACTCTGACTG-3'], approximately 100,000 water molecules, and Na^+ and Cl^- ions. Simulations were run for NaCl concentrations of 0.02 M, 0.1 M, 1.1 M, and 1.8 M. The charge of the ssDNA molecule, with 21 PO_4^- groups, was balanced by 21 additional Na^+ ions. Therefore, we defined the salt molarity as the Na^+ concentration. The system included approximately 300,000 atoms (the number of atoms change depending on the NaCl concentration).

To directly assess the effects of intermolecular interactions between neighbouring ssDNA molecules, we carried out simulations on a 2-dimensional hexagonal lattice of ssDNA molecules grafted to a surface. The CH_3 group at the end of each molecule was constrained to a plane representing the surface, with the distance between neighbouring molecules (2.73 nm) giving a surface density of 1.55×10^{13} molecules/cm^2, which is within the range of the experimental surface densities. These simulations were run at Na^+ concentrations of 0.9 M. For each simulation, we ran molecular dynamics simulations for 300 ns. The 300 ns of simulation time at each concentration was carried out as four separate 75 ns simulations, where each simulation began with a different ssDNA starting condition; the starting conditions corresponded to ssDNA lengths of 4 nm, 5 nm, 6 nm, and 7nm. The ssDNA length was defined as the distance from the terminal hydroxyl group at the 3'-end to the last carbon of the 6-carbon (C_6) linker. The simulations were carried out with GROMACS 2016.1.[23]

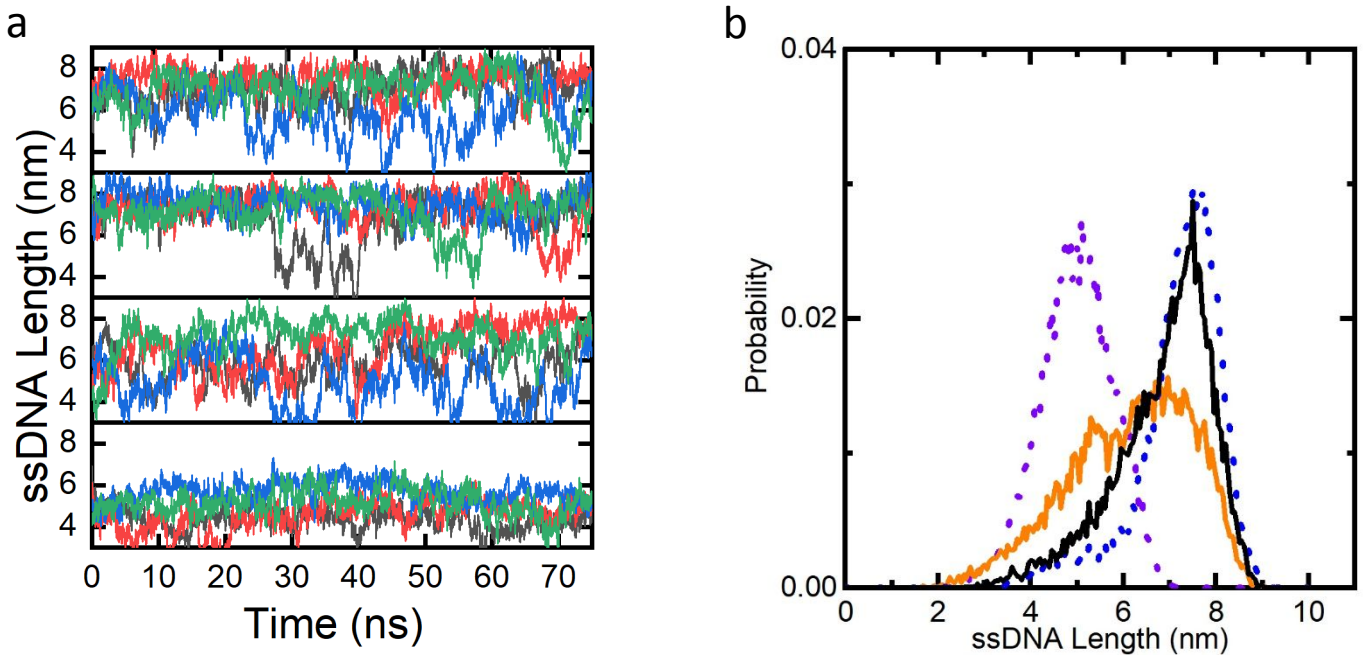

Fig. 4 (a) End-to-end distance of ssDNA through time, from top to bottom, at 0.02 M, 0.1 M, 1 M, and 2 M. **(b)** Probability distribution of the end-to-end distance for 0.02 M (solid black line), 0.1 M (dotted blue line), 1.1 M (solid orange line), and 1.8 M (dotted purple line).

Results & Discussion

Instantaneous snapshots from the molecular dynamics trajectories were visualized with Visual Molecular Dynamics.[16] **Fig. 3a** shows the ssDNA and its surroundings in 0.02 M NaCl solution. Because the ssDNA molecule has 21 PO_4^- groups that each carry a negative charge, the environment around the ssDNA molecule has more Na^+ ions than Cl^- ions, which acts to screen the charge of the ssDNA from the bulk solution.[17] The nucleic acid bases show strong tendency to stack in a straight line. **Fig. 3b** shows the ssDNA in 1.1 M NaCl solution, where there are ample amounts of both ions near the ssDNA. There are frequent disruptions of the nucleic acid base stacking at high salt concentration, such that the nucleic acids are less likely to stack in a line. This tendency is also observed with simulations of ssDNA molecules in a hexagonal lattice, as we show by comparing **Fig. 3b** and **Fig. 3c**. This result is consistent with previous findings that the end-to-end distance and the persistence length of nucleic acid strands decrease with increasing ionic strength of the solution.[15]

We show the molecular dynamics results for the ssDNA end-to-end distance as a function of time in **Fig. 4a**, where this distance is defined between the 5' PO_4^- group and the 3' PO_4^- group. The end-to-end distance fluctuates to shorter distances more frequently at higher salt concentrations. In **Fig. 4b**, we show the probability distributions of the end-to-end distances. With increasing salt concentration, the distributions shift toward shorter distances. This trend concurs with previous experimental works based on single-molecule fluorescence energy transfer (smFRET) for free ssDNA molecules suspended in solution[12] and ssDNA molecules tethered to a surface,[11] where in both cases the ssDNA becomes shorter with increasing salt concentration.

We compare our simulation end-to-end distances of a single ssDNA molecule in solution with the experimental AFM heights of high-density ssDNA brushes in **Fig. 5**. These two quantities show excellent quantitative agreement over the broad range of salt concentration tested here, in which there is a significant change in brush height. Furthermore, our simulations carried out at surface density of 1.55×10^{13} molecules/cm^2 (**Fig. 3c**), when taken in comparison to our isolated molecule results, show that the ssDNA-ssDNA interactions within the monolayer have a negligible effect on the end-to-end distance.

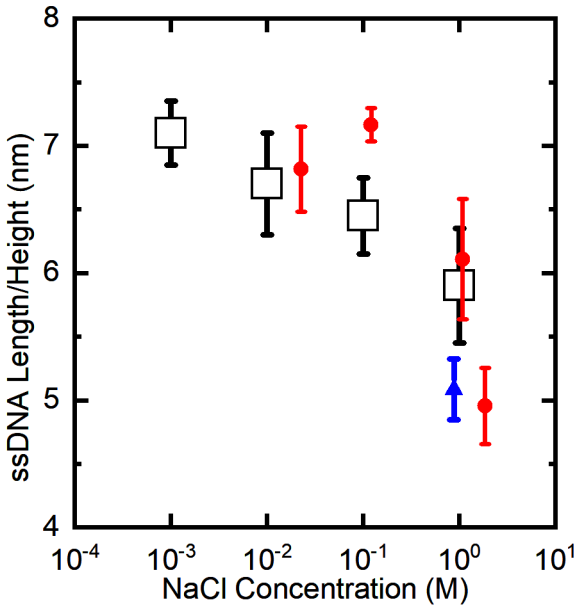

Fig. 5. The experimental AFM heights (black squares), the average ssDNA end-to-end distances at infinite dilution from simulations (red circles), and the average ssDNA end-to-end distance at surface density of 1.55×10^{13} molecules/cm^2 from simulations (blue triangle).

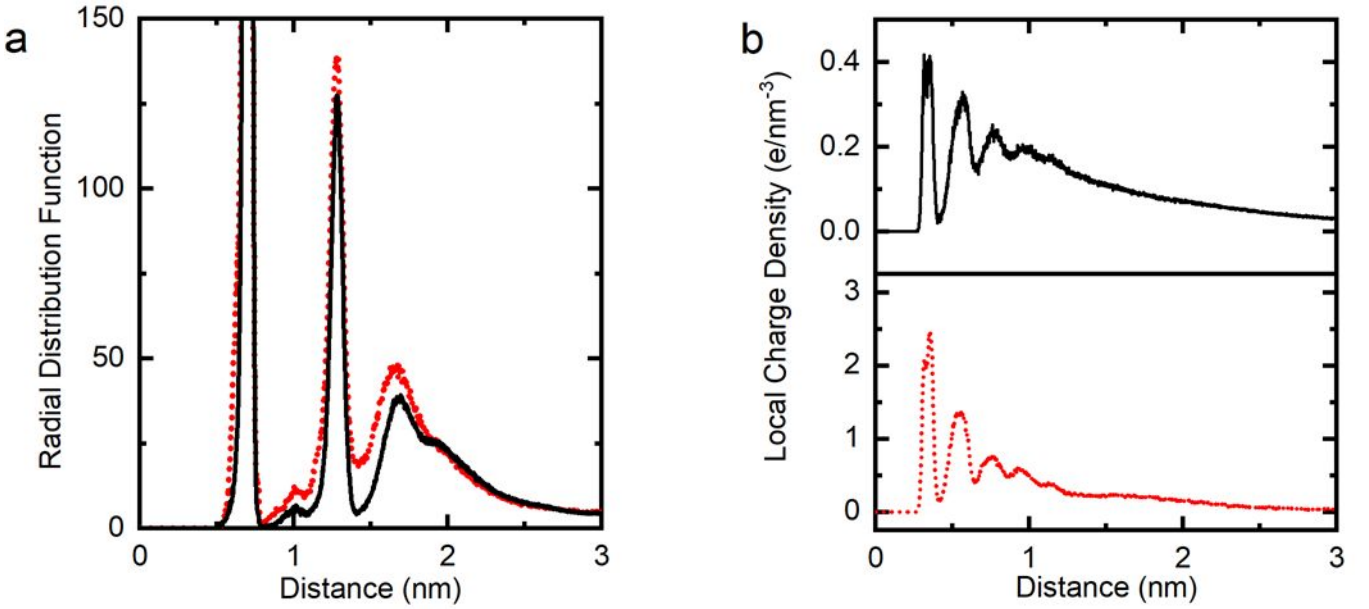

Fig. 6 (a) Phosphate-phosphate radial distribution functions, which correspond to the average local density of phosphates groups as a function of distance from a given phosphate group, normalized by the overall average density of phosphate groups. Results are shown at 0.02 M (black) and 1.8 M (red). **(b)** Average local charge density as a function of distance from a given phosphate atom at 0.02 M (top, black) and 1.8 M (bottom, red).

These results show that the intramolecular interactions within the single ssDNA molecule, mediated by the salt environment, as the factor that dominates the height of the high-density ssDNA brush. The reason for the dominance of intramolecular interactions over intermolecular interactions is two-fold: (1) Intramolecular charged groups are closer than intermolecular groups, as the distance between adjacent phosphate groups within a ssDNA molecule is ~0.7 nm while the distance between adjacent ssDNA molecules is ~2.7 nm; (2) Intramolecular charge groups will repel in the direction that stretches the molecule, while intermolecular interactions will repel in the orthogonal direction. Note the intermolecular electrostatic forces between molecules will play a role in orienting the ssDNA molecules perpendicular to the surface, as the intermolecular interactions act in the direction to push molecules apart, even though they negligibly affect the end-to-end distance of individual molecules.

To understand how the ssDNA structure changes with salt concentration, we examine the phosphate-phosphate radial distribution function as shown in **Fig. 6a** (the radial distribution function is defined in the figure caption). The first peak corresponds to nearest-neighbour phosphates, the second peak corresponds to second-nearest-neighbour phosphates, and the third peak is broad due to smearing of the third- and higher-neighbour phosphates. As the salt concentration increases from 0.02 M, the order decreases (i.e., the radial distribution function exhibits larger values between the peaks). The decreased order leads to increased flexibility, as the molecule moves between more configurations, and thus to a shortening of ssDNA molecule via increased bending and torsional movements of the ssDNA backbone. To probe the electrostatic interactions that underlie the conformational changes, we examine the net charge density (the sum of Na^+ ion and Cl^- ion local densities) as a function of the distance from the phosphate groups, as shown in **Fig. 6b**. Higher salt concentration leads to more positive charge that surround the phosphate groups, which weakens the repulsive electrostatic interactions between the phosphate groups, and allows the ssDNA to contract when the salt concentration is higher. This result concurs with previous ideas of the ion atmosphere.[25]

There has been much previous work addressing the dependence of the heights of flexible polymer brushes on salt concentration and grafting density.[2-9] The brush height of flexible polymer brushes is governed by the balance of (1) the "entropic spring" nature of polymers that acts to coil the molecule and decrease the height, and (2) the intermolecular interactions that act to uncoil the polymer and increase the height.

In contrast, the situation for ssDNA oligomers is very different. Short brushes such as ssDNA oligomers do not coil to the same extent as long flexible polymers. Rather, the ssDNA structure is more like a flexible rod (see Fig. 3). The height of ssDNA brushes is not dominated by the extent of coiling of individual strands. When the ssDNA molecules are grafted on a surface, entropic spring effects do not come in to balance intermolecular interactions, as in the case in polymer brushes. Instead, the brush height is dominated by intramolecular electrostatic interactions, in combination with intermolecular interactions which act to orient the molecules in the direction perpendicular to the surface.

Conclusions

In this work, we used a combination of experiments and molecular dynamics simulations to understand the structure of ssDNA brushes. In a brush where a high-density monolayer of ssDNA is tethered to a surface, one can expect a variety of interactions to contribute to the brush structure. We show here

that the intramolecular interactions within a single ssDNA molecule, mediated by the salt environment, dominate the end-to-end distances of individual ssDNA molecules in high-density ssDNA brush; the ssDNA-surface interactions and ssDNA-ssDNA interactions negligibly affect the end-to-end distance. The salt environment has the effect of screening the repulsive electrostatic interactions between the phosphate groups, which reduces the extent to which the ssDNA molecule is held rigidly in an elongated state, and thus leads to shortening of the molecule.

Conflicts of interest

There are no conflicts to declare.

Acknowledgements

This material is based upon work supported by the US National Science Foundation under grant number DMR-1206480 to D.J.L., the FIRB under 2011 grant "Nanotechnological approaches toward tumor theragnostic" to P.P. and L.C., the Associazione Italiana per la Ricerca sul Cancro (AIRC) under a grant to L.C. and A.B. (AIRC 5 per mille 2011, no. 12214), and the European Research Council (ERC) under the grant "Monalisa Quidproquo" to M.D.N.N. The calculations were carried out using computational resources through the Ohio Supercomputing Center. The collaboration was initiated through the Mandela Washington Fellows program, funded by grants from the US Department of State to D.J.L. and M.D.N.N.

Notes and references

1 J. J. Gooding. Electroanalysis, 2002, 14, 1149-1156
2 E. B. Zhulina, O. V. Borisov, V. A. Pryamitsyn, and T. M. Birshtein. *Macromolecules*, 1991, 24, 140-149.
3 P. Pincus. *Macromolecules*, 1975, 9, 386-388.
4 M. Biesalski and J. Rühe. *Macromolecules*, 2002, 35, 499-507.
5 B. M. Orkugin et al. *Soft Matter*, 2018, 14, 6230.
6 J. Yu et al. *Macromolecules*, 2016, 49, 5609-5617.
7 I. O. Lebedeva, E. B. Zhulina, and O. Borisov. *J. Chem. Phys.,* 2017, 146, 214901.
8 T. Wu et al. *Macromolecules*, 2007, 40, 8756-8764.
9 P. Gong, T. Wu, J. Genzer, and I. Szleifer. *Macromolecules*, 2007, 40, 8765-8773.
10 M. D. N. Ngavouka, A. Bosco, L. Casalis and P. Parisse. Macromolecules, 2014, 47, 8748-8753.
11 D. Bracha, E. Karzbrun, S. S. Dabue and R. H. Bar-Ziv. Acc. Chem. Res., 2014, 47, 1912-1921.
12 M. C. Murphy, I. Rasnik, W. Cheng, T. M. Lohman and T. Ha. Biophys. J. 2004, 86, 2530-2537.
13 M. Rueda, E. Cubero, C. A. Laughton and M. Orozco. Biophys. J. 2004, 87, 800-811.
14 H. Chen et al. PNAS, 2011, 109, 799-804.
15 E. Mirmotax et al. Nano Lett., 2008, 8, 4134-4139.
16 A. Bosco et al. Nanoscale, 2012, 4, 1734-1741.
17 I. Ivani et al. Nature Methods, 2015, 13, 55-58.
18 H. J. C. Berendsen, J. R. Grigera and T. P. Straatsma. J. Phys. Chem., 1987, 91, 6269-6271.
19 L. X. Dang. J. Am. Chem. Soc., 1995, 117, 6954-6960.
20 H. J. C. Berendsen, J. P. M. Postma, W. F. Gunsteren, A. DiNola and J. R. Haak. J. Chem. Phys., 1984, 81, 3684.
21 G. Bussi, D. Donadio and M. Parrinello. J. Chem. Phys., 2007, 126, 014101.
22 T. Darden, D. York and L. Pedersen. J. Chem. Phys., 1993, 98, 10089.
23 M. J. Abraham et al. SoftwareX, 2015, 1-2, 19-25.
24 W. Humphrey and K. Schulten. J. Mol. Graph., 1996, 14, 33-38.
25 J. Lipfert, S. Doniach, R. Das and D. Herschlag. Annu. Rev. Biochem., 2015, 83, 813-841.

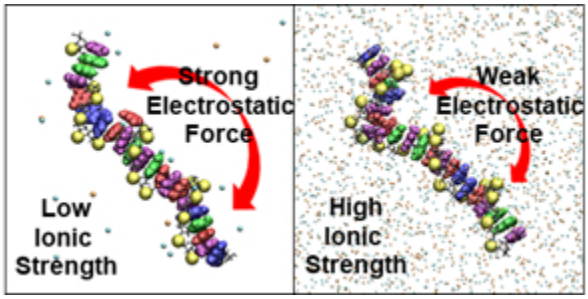

106x51mm (72 x 72 DPI)